*Journal of*
*Nanoscience and Nanotechnology*
Vol. 12, 1–7, 2012

# *Ab-Initio* Adsorption Study of Chitosan on Functionalized Graphene: Critical Role of Van Der Waals Interactions

R. Rahman[1] and D. Mazumdar[2,*]

[1] *Department of aerospace engineering and mechanics, The University of Alabama, Tuscaloosa, AL 35487*
[2] *Center for Materials for Information Technology, University of Alabama, Tuscaloosa, AL 35487*

We investigate the adsorption process of an organic biomolecule (chitosan) on epoxy-functionalized graphene using *ab-initio* density functional methods incorporating van-der-waals (vdW) interactions. The role of London dispersion force on the cohesive energy and conformal preference of the large molecule is quantitatively elucidated. Binding energy values are observed to increase by over an order of magnitude after including vdW corrections to the total energy, implying that dispersive interactions dominate the physisorption process. Functionalizing graphene with epoxy groups also leads to weak hydrogen-bond interactions with the hydroxyl and amine functional groups of chitosan. Detailed conformal study of functional groups reveal that binding is strongest when the molecule is oriented with the hydroxyl group approaching the functionalized graphene. At the binding distance a cohesive energy of nearly 30 kcal/mol is evaluated for this configuration which changes very slowly with increasing distance. Our study furthers advances the promise of functionalized graphene for a variety of applications.

**Keywords:**

RESEARCH ARTICLE

## 1. INTRODUCTION

Graphene based research is moving at a breathtaking speed ever since the ideal two-dimensional flatland was discovered in 2004.[1] The impact is such that the discoverers have been awarded the 2010 physics Nobel Prize. The unique structure of graphene with a zero band gap at Dirac point has attracted the physics community as the electronic motion is akin to a massless particle.[2] The high electronic mobility is equally attractive for a variety of electronic applications, and engineering ways to open and possibly tune the band gap by doping or structural modification[3,4] has been one of the major research thrust.

A current active topic for graphene application is in the area of biological and electrochemical sensors where it could act as an excellent electrode material. Apart from its high electrical mobility, single layer graphene has a large surface area (theoretically 2630 $m^2/g$), high mechanical strength,[5] thermal conductivity,[6] and excellent biocompatibility. Recent experiments have also demonstrated that graphene can be chemically functionalized with organic molecules, enzymes, all of which is promising for novel graphene-based biosensors and nanocomposites.[7–10] Theoretical studies using graphene as an electrode has largely focussed on chemisorption processes of small molecules like $NO_2$, $O_3$[11,12] *p*-type or monovalent elements.[13,14] But research into adsorbates which are either biological or organic is also gathering much importance. Binding of large organic bio-polymers such as polysaccharides on graphene is particularly relevant for applications such as immunoassay, drug-delivery and bio-sensing. However, for such sparse matter, the absorption process is of physical nature (physisorption) where the dominant interaction responsible for attractive forces are weak, long-ranged van-der Waals (also called dispersive London forces).[15] Traditional first-principles method implementing density functional theory use either local density or generalized gradient approximation and are primarily suited to describe the ground state of dense (solid state) matter. Therefore search has intensified in recent years looking for methods at the *ab-intio* level which can treat both local and long-ranged interactions within the same framework. From a practical stand-point, these methods can provide valuable insight into experiments which are often difficult to interpret due to a variety of factors.

*Author to whom correspondence should be addressed.

In the last decade or so, with the advent of van der waals density functional theory, a theoretical framework for investigating physisorption processes have been established[16] and is the central theme of our work here. We study the adsorption of a single repeat unit of the Chitosan (CS) molecule $[C_6H_{12}NO_5]_n$ $(n = 1)$ on functionalized graphene with corrections to include non-local Van-der waals dispersion forces. CS is a promising biodegradable, non-toxic, natural biopolymer with multiple functional groups such as the amine ($NH_2$), and hydroxyl (OH). CS is generally obtained by deacetylation of chitin, which is one of the most abundant natural occurring polymer on earth. Recently, CS has also attracted significant interest in a broad range of biological applications including as tissue engineering, and drug delivery.[17] Another motivation for this work is an attempt to understand if graphene platelets are well dispersed (not to be confused with dispersion forces) in the CS solution in order to achieve reasonable effect of nano-reinforcement in different applications. Compared to pristine graphene, graphene-oxide (GO) is expected to have better dispersion in aqueous CS solution.[8] In this study, both pristine graphene (GN) and epoxy-group functionalized graphene plates (FGN) were investigated.

## 2. COMPUTATIONAL DETAILS

In this work *ab-initio* density functional calculations were carried out using the Vienna *ab-initio* simulation package (VASP).[18, 19] To include long-range van der Waals interaction to the total energy of the system we have adopted the approach proposed originally by Dion et al.[16] where perturbative corrections to the local or semi-local DFT electronic density (say, using, the Generalized Gradient Approximation (GGA)) attributes for non-local correlations. Specifically for this work we have used this approach as implemented in the Junolo package.[20] In the next section, we describe the essential elements of van der Waals density functional theory. Detailed description of the method can be found in the pioneering 2004 works of Dion et al.[16, 21] and later in Thonhauser et al.[22] One advantage of this formalism is that it does not need to be modified (in a strict sense) for systems where non-local corrections are comparatively smaller.

### 2.1. Theoretical Background

Van der Waals (VdW) interaction leading to dispersive (London) forces arise from quantum (or thermal) fluctuations of dipoles, which results in an attractive force with long-range $d^{-6}$ dependence. These dynamic correlation effects can be treated, in principle, from ground state calculations of exact density functional theory (DFT). However, approximations to DFT such as local density approximation (LDA) or semi-local Generalized Gradient approximation (GGA) fail to incorporate long-ranged VdW interactions due to their intrinsic local (or semi-local) nature. These approximation can best describe cases where the electronic densities strictly overlap (like covalent bonding for example). However, it has been noted that GGA-type functionals can reproduce an attractive interaction from exchange interactions only. But in reality this has nothing to do with VdW, which is strictly a correlation effect.[23]

For a proper theoretical framework, it is important to separate out the exchange and correlation part from the exchange-correlation functional and treat them separately as approximations.

$$E_{xc} = E_x + E_c \tag{1}$$

where $E_{xc}$ is the exchange-correlation functional in DFT and $E_x$ and $E_c$ are its exchange and correlation sub-parts.

We can now split the correlation functional $E_c$ into two parts as

$$E_c = E_c^L + E_c^{NL} \tag{2}$$

where the long-ranged terms giving rise to vdW ($E_c^{NL}$) are separated from the semi long-ranged terms ($E_c^L$).[21] Further it can be argued in the limit of slowly varying systems $E_c^L$ is best approximated by LDA-correlation, $E_c^{LDA}$.[21] Therefore, the correlation functional term is written as

$$E_c = E_c^{LDA} + E_c^{NL} \tag{3}$$

This is not to say that we cannot use GGA exchange-correlation functionals (like PBE for instance). Fortunately, in principle, one has only to subtract out the GGA-correlation energy to avoid counting this term twice. In such a case the total energy becomes

$$E_{total} = (E_{total}^{GGA} - E_c^{GGA} + E_c^{LDA}) + E_c^{NL} \tag{4}$$

where $E_{total}$ is the ground state energy with the non-local energy contribution included ($E_c^{NL}$). $E_{total}^{GGA}$ is the total ground state energy using only GGA exchange-correlation functional, and $E_c^{GGA}$ is the GGA correlation sub-part of $E_{total}^{GGA}$. In doing this, we have retained the GGA exchange contribution but replaced the correlation part as in Eq. (3).

Within this frame-work, the only new formalism that needs to be developed is the approximate form of the $E_c^{NL}$ interaction. In Ref. [22], Thonhauser et al. have shown explicitly that $E_c^{NL}$ has a compact form given by

$$E_c^{NL} = \frac{1}{2}\iint d^3r d^3r' n(r)\phi(r, r')n(r') \tag{5}$$

This nonlocal correlation energy is dependent on GGA charge density $n(r)$ and the kernel $\phi(r, r')$ which depends on $|r - r'|$, electronic densities $n$ and their gradients. The kernel is computationally evaluated[16] and implemented in the Junolo package[20] used in the present work.

### 2.2. Description of System

To calculate the binding energy we use the following simple procedure: The binding energy ($E_{\text{Binding}}$) is calculated by subtracting the energy of the graphene-chitosan interacting system ($E_{\text{CS+GN/FGN}}$) from the energy of its constituents (denoted by $E_{\text{CS}}$ and $E_{\text{GN/FGN}}$ respectively) and can be simply expressed as:

$$E_{\text{Binding}} = E_{\text{CS+GN/FGN}} - E_{\text{CS}} - E_{\text{GN/FGN}} \tag{6}$$

In this work, binding energies were evaluated systematically as a function of distance between the chitosan molecule and graphene (or functionalizd graphene as the case may be). Non-local corrections, as needed by Eq. (4), were applied to this combined interacting system. Non-local corrections to the pristine as well as functionalized graphene or only chitosan in the unit cell were not considered as it adds only a constant value to the to all binding energy (which is physically irrelevant). For comparison, PBE binding energy curves were also evaluated and reported here.

Chitosan (CS) molecule $[C_6H_{12}NO_5]_n$ $(n = 1)$ structure was optimized separately using a molecular statics scheme with a steepest decent algorithm and force convergence criteria of 0.1 kcal/molÅ. The schematic diagram of the optimized structure is shown in Figure 1(i). It contains the carbon ring with functional groups attached to four of the five C-atoms. Three of them are the amine ($NH_2$) group and the other being hydroxyl (OH). A planar view of the molecule shows a layer of Hydrogen to lie above and below the plane of the ring. With this structure in mind, we have considered three different configurations of the monomer in order to orient the amine, hydroxyl and the hydrogen layer closest to the substrate. All three orientations are shown in Figure 1(v) along with the functionalized graphene sheet. These three configurations are named as:

- CHT-1: Hydrogen terminated sites closest to graphene (GN) or functionalized graphene (FGN)
- CHT-2: OH terminated sites closest to GN or FGN
- CHT-3: $NH_2$ terminated sites closest to GN or FGN

The distances reported in this work are measured with respect to the graphene sheet and the principle atom in the chitosan functional group (O for OH, N for $NH_2$ termination) as shown in Figure 1(v). It is already well established[24] that functionalized graphene is chemically more reactive than pristine graphene. The main functionalized groups are epoxy (1,2-ether, not 1,3-ether) and hydroxyl groups. In this work we have functionalized graphene with only epoxy group. Using carbon–oxygen bond distances from the paper by Yan and co-workers and others,[24] we have optimized the structure using molecular statics scheme, similar to the method adopted in optimizing chitosan . In the final structure, the oxygen is bonded with two carbon atoms at 1.9 Å from the graphene surface and located perpendicular to the graphene sheet. Experimental lattice parameters were used to generate graphene supercells (C—C bond length = 1.42 Å, in plane lattice, $a = b = 2.46$ Å). The SCF calculation was performed using the Generalized Gradient Approximation (GGA)[25] with augmented-plane wave method (PAW) with a $7 \times 7 \times 1$ Monkhorst-Pack k-point mesh and a 950 eV plane-wave cutoff. These set of parameters generated the right band structure for the 2-atom primitive graphene cell

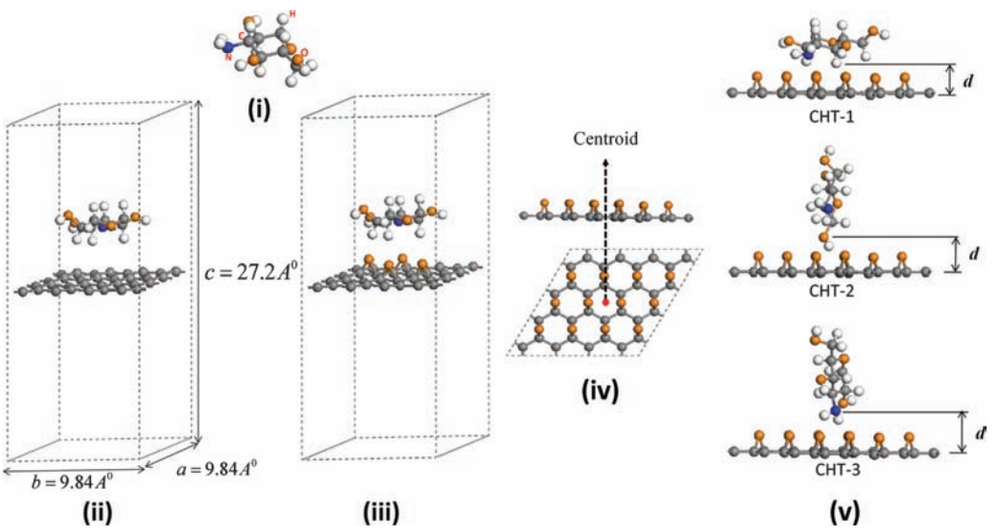


**Fig. 1.** (i) The ball and stick diagram of the optimized CS monomer ($[C_6H_{12}NO_5]_n$ $(n = 1)$). (ii) Schematic diagram of the chitosan molecule on $4 \times 4$ pristine graphene (GN) supercell. (iii) Schematic diagram of the chitosan molecule on $4 \times 4$ epoxy group functionalized graphene (FGN) optimized supercell. (iv) The centroidal axis of graphene is shown where the chitosan molecule is placed directly over in the three orientations as shown in (v). (v) Three orientations of chitosan molecule on epoxy-functionalized graphene surface with H-termination (CHT-1), OH-termination (CHT-2), and $NH_2$-termination (CHT-3) at a distance $d$ from the graphene plane. This distance is varied to obtain the results.

(consistent with literature reports) and also for larger $2 \times 2$, $4 \times 4$ and $8 \times 8$ supercells. The cut-off radii (in units of Angstroms) of 0.77, 0.546, 0.549, and 0.472 were defined for C, O, N and H respectively.

The supercells of GN as well as FGN are shown in Figures 1(ii) and (iii). The centroid of the chitosan monomer was made coincident with the centroid of the graphene sheet as shown in Figure 1(iv). A $4 \times 4$ (32 atom) graphene supercell was necessary to prevent spurious self-interaction of the large chitosan monomer due to cell periodicity. A large vertical distance of $c = 27.2$ Å between the GN and FGN sheets ensured that the interaction energy could be evaluated over a large distance and for all the orientations. As a result, the graphene layer or CS were also separated enough in adjacent cells to discard the effect of nonlocal interactions. Using this supercell, dipole energy corrections were found to be negligable in comparison with other energies values we report here.

## 3. RESULTS

In Figure 2, we plot the GGA(PBE)-derived binding energy as a function of distance between pristine graphene and CS in the three configurations of the organic molecule. The interaction curves closely represent Lennard-Jones type[14, 15] where at very small length scales (less than 1.5 Å) the interaction is repulsive, reaches a stable minima (binding configuration) at an intermediate value (1.5–2.0 Å), and asymptotically approaches zero at large distances (above 3.5 Å) (2). The summary for this calculation is shown in Table I – Case 1. We find that the binding energy value is about 1 kcal/mol on an average, and slightly higher for Hydrogen (CHT-1) termination at 1.4 kcal/mol than hydroxyl (CHT-2) and amine termination (CHT-3). The binding distance is also lower for Hydrogen

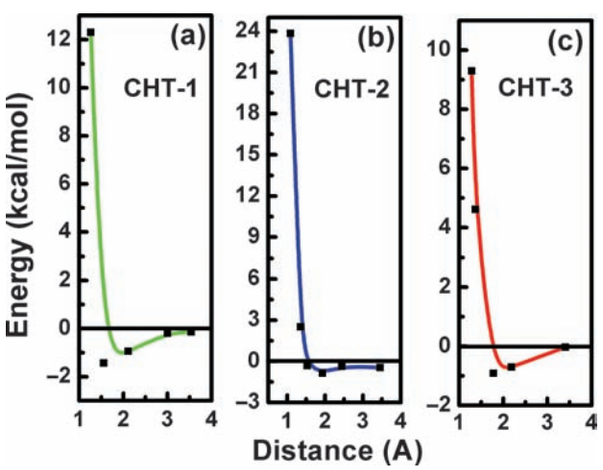


**Fig. 2.** Binding energy versus separation curve for the three different orientations of CS molecule on pristine graphene with GGA (PBE) functional. Some data points in the repulsive regime are not shown (out of scale) for better clarity.

**Table I.** Binding energy and distance for different cases.

| Calculation scheme | Orientation | Binding energy (kcal/mol) | Binding distance (Å) |
|---|---|---|---|
| Case-1 | CHT-1 | 1.43 | 1.55 |
| | CHT-2 | 0.90 | 1.77 |
| | CHT-3 | 0.90 | 1.77 |
| Case-2 | CHT-1 | 1.98 | 1.90 |
| | CHT-2 | 2.87 | 1.71 |
| | CHT-3 | 2.26 | 2.20 |
| Case-3 | CHT-1 | 13.63 | 1.56 |
| | CHT-2 | 28.87 | 1.61 |
| | CHT-3 | 10.85 | 1.90 |

*Notes*: [1] Case-1: CS on GN and PBE [2] Case-2: CS on FGN and PBE [3] Case-3: CS on FGN and PBE + nonlocal correlation.

termination (CHT-1 case, 1.5 Å vs. 1.8 Å). As noted in the paper by Xu and co-researchers,[23] this apparent binding could originate from exchange interactions only and may not reflect the true long-ranged van der Waals interaction at all. We therefore refer to this binding as GGA-binding from now on.

We next proceeded to investigate binding with functionalized graphene still within the realm of semi-local GGA. We found the PBE binding energy values to improve substantially after functionalizing graphene with epoxy as shown in Figures 3(a)–(c) for all the three cases and the results are summarized in Table I – Case 2. Compared to pristine-graphene case, the binding distance is larger by nearly 0.5 Å for CHT-1 and CHT-3 as the presence of epoxy ions on the graphene surface forces the chitosan molecule in these orientations to be further away from the graphene plane in order to avoid strong electrostatic repulsion. However, CHT-2 (hydroxyl) orientation does not follow this trend and the binding distance is slightly lower compared to pristine-graphene case (1.77 Å vs. 1.71 Å). This can be explained by noting that the hydroxyl group is much smaller in terms of spatial extension and therefore the chitosan molecule, in this case, can approach the graphene surface without getting close to the epoxy molecules. The binding energy is also highest for the CHT-2 orientation with an improvement of nearly 2.0 kcal/mol compared to GGA-binding, followed by the CHT-3 (amine) orientation (1.5 kcal/mol), whereas for the Hydrogen (CHT-1) termination the increase is only modest 0.5 kcal/mol. This increase cannot be accounted by changes in GGA-binding, if at all, and strongly suggests that some other interaction is at play due to the presence of epoxy-oxygen. A careful look into the geometry of these configurations (Fig. 1(v)) reveals that hydrogen bonding is the most likely interaction. The terminal H-ion of the OH or $NH_2$ functional group is closer to some of the epoxy-oxygen ions on the graphene surface, which creates a favorable situation for the electronic lone pair in the epoxy-oxygen molecule to interact with the the polar hydrogen ion in the OH and $NH_2$ functional group of

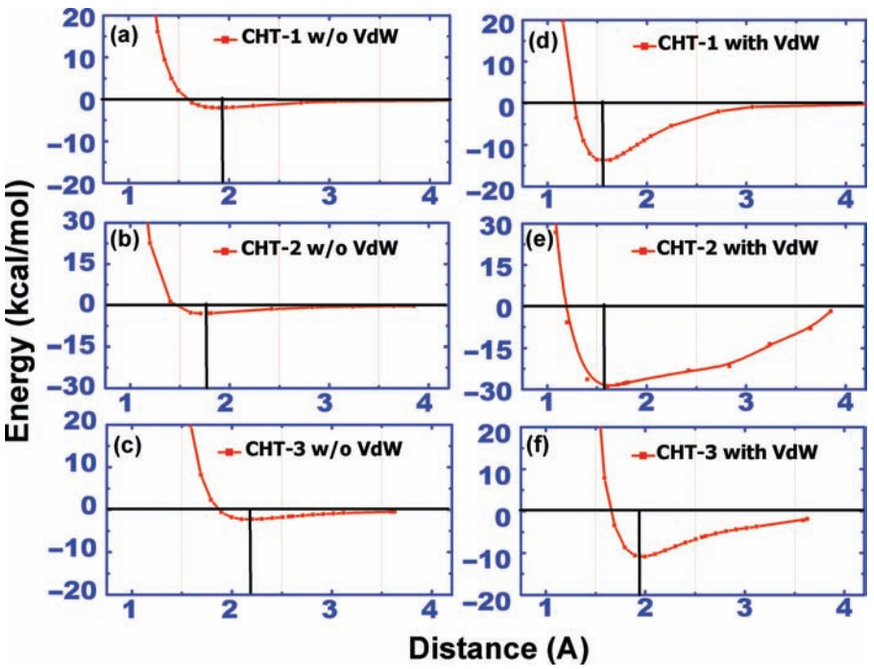


**Fig. 3.** Binding energy versus separation curve for the three different orientations of CS molecule on functionalized graphene (FGN) without (a–c) and with (d–f) van der Waals interaction. Dashed line show position of the binding distance.

the type O...H-X (X = O, N). From a formal point-of-view, hydrogen bonding is known to be captured within GGA[26, 27] which gives us added confidence. It is however complicated by the fact that the bonds are non-linear, much less than 180°, which weakens hydrogen bonding.[28] To show the presence of lone pairs—which are necessary for hydrogen bonds between functionalized graphene and chitosan—we plot explicitly the electron localization function (ELF)[29] in Figures 4((a)–(c)). Electron localization function is a measure of non-bonding electron pair, and was originally proposed by Becke and Edgecombe.[29] The location where ELF attains values close (or equal to) 1.0 is a quantitative signature of lone pair. In Figure 4, the presence of lone pairs with opposite spin in the oxygen molecule of the epoxy group is clear with ELF values approaching 0.9 (red). In close proximity of the epoxy-oxygen we also observe lone pairs in chitosan molecule. So all the evidence points to hydrogen bonding being responsible for the enhanced binding with chitosan from adding the epoxy molecules to the graphene substrate.

Binding energy curves after including non-local van der Waals corrections are shown in Figures 3(d)–(f) and summarized in Table I – Case 3. Almost or over an order of magnitude difference in energy is observed compared to GGA (case 2). The highest increase is observed for the case of OH functional group (CHT-2) where the binding energy approaches almost 30 kcal/mol. In the case of $NH_2$ (CHT-3) and H (CHT-1) termination, the binding energy values are between 10–13 kcal/mol. Apart from the dramatic increase in the binding energy value, the inclusion of non-local corrections also brings out a clear conformal



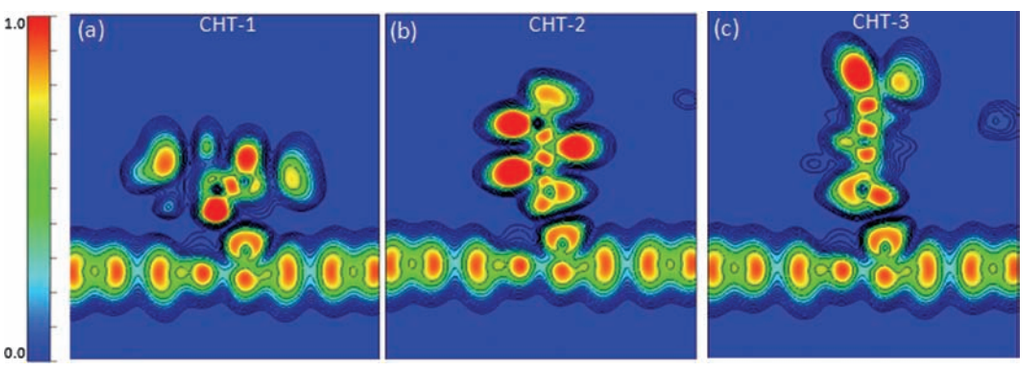


**Fig. 4.** (a)–(c): Electron localization function of the functionalized graphene-chitosan system showing the location of non-bonding lone pairs (red).

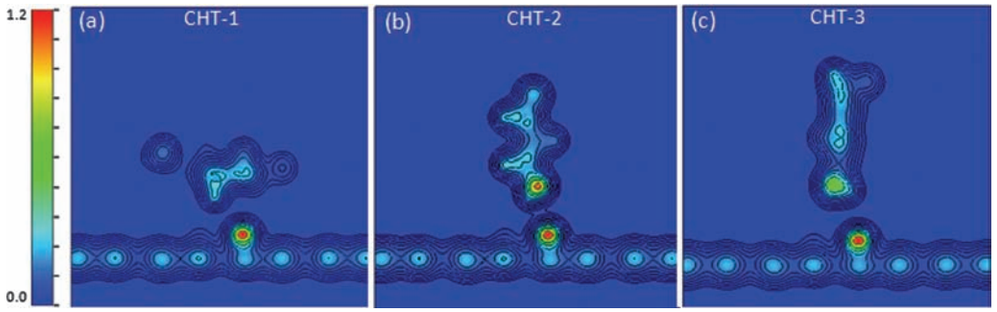


**Fig. 5.** (a)–(c): Charge density isosurfaces along the (110) plane for the three different orientations of CS molecule on functionalized graphene (FGN) at the binding distance.

preference of the interacting system, with the CHT-2 case overwhelmingly being the orientation with highest binding energy for the physiosorption process. Further, we observe that large binding energy values for the CHT-2 orientation is sustained for over a large distance between the OH site and the nearest oxygen ion on the fucntionalized graphene substrate. This can be quantitatively estimated by the distance over which the binding energy is half the maximum value, the so-called full-width-at-half-maximum (FWHM). FWHM value is close to 1.3 Å for CHT-2 (OH) orientation, whereas for CHT-3 ($NH_2$) case it is slightly lower at 0.8 Å, and for CHT-1 (H-termination) case it is 0.4 Å. This highlights that apart from the higher binding energy, the physiosorption process can remain mobile over an appreciable distance for the CHT-2 orientation. We also observe a slight decrease in the binding distance compared to PBE binding (case 2 vs. case 3 in Table I), which again points to greater attraction from non-local interaction and also consistent with the observation of Wu et al.[29]

While it is difficult to pinpoint the reason explaining the conformal preference, we speculate that the large organic molecule (chitosan) is easily polarizable along certain directions and the induced dipole moment is highest for CHT-2 orientation of the molecule. Anisotropic polarizability is not unusual among organic molecules with different bonding in different directions and, mathematically, static polarizability is described by a tensor. Therefore it is quite plausible to assume that the induced dipoles—which causes London dispersion forces—will exhibit similar anisotropic behavior. A detailed investigation is beyond the scope of the present work and will be a subject of a future effort.

To further investigate differences between CHT-2 and other orientations, we investigated the PBE-GGA valence charge density at the optimum binding energy distance for all three conformal orientations (Figs. 5(a)–(c)). The charge density slices shown in the figure are in the (110) plane of the unit cell. The maps are shown in Red-Yellow-Blue (RYB) color scheme where red implies maximum electron density, blue the minimum. Charge density contours (isosurfaces), plotted in logarithmic scale, depict variation by two orders of magnitude. Blue, contour-less regions, are areas where the electronic charge density is less than 1% of the values encountered for the core electrons (red regions). As evident in the charge contour plots, we observe that only in the case of OH termination (CHT-2), the charge density in the region between the molecule and substrate does not fall below 1% of the maximum value, where as in the other two cases there is no charge density overlap. Similar results were obtained for slices viewed in other planes. We believe that the proximity of the charge densities could also lead to higher van der Waals attraction—albeit in a much local scale—for the case of CHT-2 orientation.

## 4. CONCLUSIONS

In summary, we have investigated the binding of a prototypical biomolecule (chitosan) on graphene functionalized with epoxy molecules within the framework of van der Waals density functional theory. We find evidence of, and obtain quantitative estimates of binding due to long-range induced dipole interactions leading to dispersion forces, and static dipole interaction leading to hydrogen bonding. Our calculations reveal that the physisorption process is entirely dominated by non-local London dispersive forces with hydrogen bonding playing a much weaker, but substantial, role after functionalizing graphene with epoxy molecules due to the presence of O...H-X (X = N, O) bonds. A strong conformal preference is also obtained in our calculations—the configuration where the chitosan molecule is orientated with the hydroxyl group closest to the substrate is heavily favored with a binding energy of nearly 30 kcal/mol—which is more than double than the other orientations considered in this work. Also the decrease of the binding energy with distance is much slower for this orientation.

## References and Notes

1. K. S. Novoselov, A. K. Geim, S. V. Morozov, D. Jiang, Y. Zhang, S. V. Dubonos, I. V. Grigorieva, and A. A. Firsov, *Science* 306, 666 (**2004**).
2. A. K. Geim and K. S. Novoselov, *Nat. Mater.* 6, 183 (**2007**).

**3.** M. Y. Han, B. Ozyilmaz, Y. Zhang, and P. Kim, *Phys. Rev. Lett.* 98, 206805 **(2007)**.
**4.** Y. Zhang, T.-T. Tang, C. Girit, Z. Hao, M. C. Martin, A. Zettl, M. F. Crommie, Y. R. Shen, and F. Wang, *Nature* 459, 820 **(2009)**.
**5.** C. Lee, X. D. Wei, J. W. Kysar, and J. Hone, *Science* 321, 385 **(2008)**.
**6.** S. Park and R. S. Ruoff, *Nat. Nanotechnology* 4, 217 **(2009)**.
**7.** S. Stankovich, D. A. Dikin, G. H. B. Dommett, K. M. Kohlhaas, E. J. Zimney, E. A. Stach, R. D. Piner, S. T. Nguyen, and R. S. Ruoff, *Nature* 442, 282 **(2006)**.
**8.** X. Yang, Y. Tu, L. Li, S. Shang, and X.-M. Tao, *ACS Applied Materials and Interfaces* 2, 1707 **(2010)**.
**9.** M. S. Xu, D. Fujita, and N. Hanagata, *Small* 5, 2638 **(2009)**.
**10.** N. Mohanty and V. Berry, *NanoLetters* 8, 4469 **(2008)**.
**11.** T. O. Wehling, K. S. Novoselov, S. V. Morozov, E. E. Vdovin, M. I. Katsnelson, A. K. Geim, and A. I. Lichtenstein, *NanoLetters* 8, 173 **(2008)**.
**12.** G. Lee, B. Lee, J. Kim, and K. Cho, *J. Phys. Chem. C* 113, 14225 **(2009)**.
**13.** O. U. Akturk and M. Tomak, *Appl. Phys. Lett.* 96, 81914 **(2010)**.
**14.** E. Akturk, C. Ataca, and S. Ciraci, *Appl. Phys. Lett.* 96, 123112 **(2010)**.
**15.** J. E. Lennard-Jones, *Proc. R. Soc. Lond. A* 106, 463 **(1924)**.
**16.** M. Dion, H. Rydberg, E. Schroder, D. C. Langreth, and B. I. Lundqvist, *Phys. Rev. Lett.* 92, 246401 **(2004)**; M. Dion, H. Rydberg, E. Schroder, D. C. Langreth, and B. I. Lundqvist, *Phys. Rev. Lett.* 95 109902E **(2005)**.
**17.** P. M. Kumar, *React, Funct. Polym.* 46, 1 **(2000)**.
**18.** G. Kresse and J. Furthmuller, *Comput. Mater. Sci.* 6, 15 **(1996)**.
**19.** G. Kresse and D. Joubert, *Phys. Rev. B* 59, 1758 **(1999)**.
**20.** P. Lazic, N. Atodiresei, M. Alaei, V. Caciuc, S. Blugel, and R. Brako, *Computer Physics Communications* 181, 371 **(2010)**.
**21.** D. C. Langreth, M. Dion, H. Rydberg, E. Schroder, P. Hyldgaard, and B. I. Lundqvist, *International Journal of Quantum Chemistry* 101, 599 **(2005)**.
**22.** T. Thonhauser, V. R. Cooper, S. Li, A. Puzder, P. Hyldgaard, and D. C. Langreth, *Phys. Rev. B* 76, 125112 **(2007)**.
**23.** X. Wu, M. C. Vargas, S. Nayak, V. Lotrich, and G. Scoles, *J. Chem. Phys.* 115, 8748 **(2001)**.
**24.** J.-A. Yan and M. Y. Chou, *Phys. Rev. B* 82, 125403 **(2010)**; Lerf, H. He, M. Forster, and J. Klinowski, *J. Phys. Chem. B* 102, 4477 **(1998)**; H. He, J. Klinowski, M. Forster, and A. Lerf, *Chem. Phys. Lett.* 287, 53 **(1998)**.
**25.** J. P. Perdew, K. Burke, and M. Ernzerhof, *Phys. Rev. Lett.* 77, 3865 **(1996)**.
**26.** E. E. Dahlke and D. G. Truhlar, *J. Phys. Chem. B* 109, 15677 **(2005)**.
**27.** B. Santra, A. Michaelides, and M. Scheffler, *J. Chem. Phys.* 127, 184104 **(2007)**.
**28.** J. Ireta, J. Neugebauer, and M. Scheffler, *J. Phys. Chem. A* 108, 5692 **(2004)**.
**29.** A. D. Becke and K. E. Edgecombe, *J. Chem. Phys.* 92, 5397 **(1990)**; A. Savin, A. D. Becke, J. Flad, R. Nesper, H. Preuss, and H. G. von Schnering, *Angew. Chem. Int. Ed. Engl.* 30 409 **(1991)**; B. Silvi and A. Savin, *Nature* 371, 683 **(1994)**; A. Savin, B. Silvi, F. Colonna, *Can. J. Chem.* 74, 1088 **(1996)**; A. Savin, R. Nesper, S. Wengert, and T. Faassler, *Angew. Chem. Int. Ed. Engl.* 36, 1809 **(1997)**; D. Marx and A. Savin, *Angew. Chem. Int. Ed. Engl.* 36, 2077 **(1997)**.


Received: 12 June 2011. Accepted: 07 September 2011.